

Empirical models for drop-size-dependent clustering in clouds

Alexander Marshak¹, Yuri Knyazikhin², Michael Larsen³, and Warren Wiscombe¹

¹NASA – Goddard Space Flight Center, Climate and Radiation Branch, MD

²Department of Geography, Boston University, Boston, MA

³Department of Physics, Michigan Technological University, Houghton, MI

Correspondence

Alexander Marshak

email: Alexander.Marshak@nasa.gov

Prepared for publication in

Journal of the Atmospheric Sciences

Submitted: February – 5 – 2004

Revised: June – 4 – 2004

Abstract

By analyzing aircraft measurements of individual drop sizes in clouds, it has been shown (Knyazikhin et al., 2004) that the probability of finding a drop of radius r at a linear scale l decreases as $l^{D(r)}$ where $0 \leq D(r) \leq 1$. This paper shows striking examples of the spatial distribution of large cloud drops using models that simulate the observed power laws. In contrast to currently used models that assume homogeneity and a Poisson distribution of cloud drops, these models illustrate strong drop clustering, the more so the larger the drops. The degree of clustering is determined by the observed exponents $D(r)$. The strong clustering of large drops arises naturally from the observed power-law statistics. This clustering has vital consequences for rain physics, including how rain can form so fast. It also helps explain why remotely sensed cloud drop size is generally larger than measured in situ and why clouds absorb more sunlight than conventional radiative transfer models predict.

1. Introduction

Though it is widely assumed that cloud drops are distributed uniformly in space and fluctuations of number of drops in a given small volume follow Poisson statistics (e. g., Young, 1993), there is strong evidence of cloud drop clustering on a wide range of scales down to centimeter scales (e.g., Hobbs and Rangno, 1985; Baker, 1992; Pinsky and Khain, 2001, 2003; Kostinski and Jameson, 1997; Jameson et al., 1998; Davis et al., 1999, Shaw et al., 2002). Clustering can be identified as significant fluctuations in cloud drop concentration (Jameson et al., 1998) defined as the expectation of the number of drops per volume when volume tends to 0 (Pawlowska and Brenguier, 1997). Analyzing Forward Scattering Spectrometer Probe (FSSP) data Baker (1992) reported a deviation from a Poisson distribution which is characterized by a perfectly random spatial distribution. Pinsky and Khain (2001) studied the fine structure of cloud drop concentrations using Fast FSSP (Brenguier et al., 1998) measurements; they showed that the degree of drop concentration fluctuations strongly depends on the drop size. Later Pinsky and Khain (2003) found that drop clusters on cm-scales are induced by droplet inertia within turbulent flow. Thus, small-scale drop variability carries information about the fine structure of clouds. Davis et al. (1999) assumed scale-invariance in cloud liquid water and used fractal characteristics to describe its spatial variability on scales from cm to hundreds of meters, while Jameson et al. (1998) and Kostinski and Jameson (2000) studied fluctuations of the number of 50 μm diameter cloud drops per liter using pair-correlation functions. Recently Shaw et al. (2002) argued that the pair-correlation function is the most natural and physically meaningful measure of correlations.

Liu and Hallett (1998) and Liu et al. (2002) looked at the problem from another angle: they pointed out that cloud drop size distribution is not a scale independent function but strongly depends on spatial scale over which the drops are sampled. However, as suggested by Liu et al. (2002), there is a saturation scale larger than which observed drop size distributions are scale independent. For scales smaller than the saturation scale, the drop size distribution is “ill-defined” and changes substantially from scale to scale. They hypothesized that the unique property of scale dependence requires a new theoretical framework that treats the scale as an independent variable, just as the variables of space and time are treated in the current framework. Such a parameterization, for example, may result in a better representation of clouds in climate models than complicated models with detailed microphysics because of the large range of scales involved (Liu et al., 2002).

Knyazikhin et al. (2004) proposed a way to quantitatively parameterize cloud drop clustering as a function of drop size. They suggested that number of drops is scale-invariant and follows a power law with a drop-size dependent exponent (Wiscombe et al., 2003). The clustering arises naturally from the power-law statistics and thus the drop-size dependent exponents can be used for its parameterization. Finally, using this parameterization, they estimated the direct impact of the small-scale spatial variability of drops on radiative transfer, concluding that current radiative transfer theory underestimates the effect of large drops on cloud optical depth (Knyazikhin et al., 2004).

The present paper compliments the Knyazikhin et al. (2004) results in two ways: (i) it verifies their findings of a power-law variation in cloud drop number using much more FSSP

samples acquired during the ARM Cloud Intense Operational Period (IOP) and (ii) based on these observations, it develops a method for generating spatial distribution of drops with the observed magnitude of clustering.

Understanding of spatial distribution and small-scale fluctuations (inhomogeneity) of large drops in clouds is essential to both cloud physics and atmospheric radiation communities. For cloud physics, it relates to the coalescence growth of raindrops (Twomey, 1976) while for radiation it has a strong indirect influence on the radiative properties of clouds through a rapid modification of the cloud drop size distribution and directly through changing optical path length (Knyazikhin et al., 2004).

2. Small-scale cloud drop size variability

The analyses of the FSSP data acquired during the First International Satellite Cloud Climatology Project (ISCCP) Regional Experiment (FIRE) in July 1987 indicates that the total number $N(r,l)$ of samples at a linear scale l containing drops of radius r follows a power law with a drop-size dependent exponent $D(r)$, i.e., (Knyazikhin et al., 2004)

$$N(r,l) \propto l^{-D(r)}. \quad (1)$$

The exponent $D(r)$ is a non-increasing function of the drop size r and varies between 1 (for small drops) and 0 (for very large drops). If $D(r) = 1$, drops “densely fill” the space they occupy and

the number of “nonempty” samples at a linear scale l is inversely proportional to l and the total number of drops is proportional to l^3 . The case $D(r) = 0$ corresponds to a few sparsely distributed individual drops. For $0 < D(r) < 1$, the frequency of occurrence of drops decreases with the drop-size r ; in other words, the probability of finding a drop of radius r at a linear scale l is proportional to $l^{D(r)}$.

To illustrate Eq. (1), Fig. 1 shows variation in $N(r,l)$ for $r = 7 \pm 2 \mu\text{m}$ and $r = 23 \pm 2 \mu\text{m}$ derived from data acquired during a 2-hour flight on March 3, 2000 in Kansas and Oklahoma as part of the ARM Cloud IOP (Dong et al., 2002). It is clearly seen that for a scale range of almost 3 orders of magnitude (from 80 m up to 50 km), the total number of samples with drops follows a power law with exponents $D \approx 1$ and $D \approx 1/2$ for small ($r = 7 \mu\text{m}$) and large ($r = 23 \mu\text{m}$) drops, respectively. Figure 2 shows variation in the concentration of small and large drops in 80-m intervals along the flight path. One can see that while small drops are more likely unclustered, large drops are positively clustered, (i.e., detecting a drop makes it more likely that the next drop will be detected nearby). This suggests that the deviation of the exponent from unity indicates a clustering in drop spatial distribution.

What is the importance of Eq. (1) deduced from the analysis of FSSP drop size distributions ? It follows from this equation that

- in contrast to the underlying assumption of radiative transfer theory, the mean number of drops is proportional to the drop size dependent power of the volume (Wiscombe et al., 2003);

- such behavior can not be described by a density distribution function used in data analysis; a cumulative distribution function should be used instead (Knyazikhin et al., 2002);
- there are more large drops at small scales than the theory currently accounts for; their radiative impact is consequently underestimated (Knyazikhin et al., 2004).

In the next section we show how one can simulate the spatial distribution of drops that follow a power law (1) with a given exponent. The case $D(r) = 1$ for small drops is well documented in the literature – the drop distribution can be simulated by a Poisson distribution with a given density. The spatial distribution of very large drops with exponent $D(r) = 0$ is trivial: there are a few (if any) single drops randomly located. Therefore, we will focus here on large drops with exponents $0 < D(r) < 1$.

3. Simulation

The most natural way to simulate spatial distribution of drops with scaling properties satisfying Eq. (1) is to use a threshold defined by a parameter D in turbulence cascade models. It is known (e.g., Schertzer and Lovejoy, 1989; Chhabra et al., 1989) that the probability of a d -dimensional cascade field φ_l at scale l to exceed a singularity of order γ is proportional to l^{d-D} , that is

$$Prob(\varphi_l \geq l^\gamma) \propto l^{d-D}. \quad (2)$$

Here D and γ are nontrivially related; namely, $D = D(\gamma)$ is the fractal dimension of the subset of φ_l with singularity strength γ . Indeed, if both parts of Eq. (2) are multiplied by the total number of boxes, $1/l^d$, then on the left side one gets the number of boxes with singularity strength between γ and $\gamma+\Delta\gamma$, while on the right side it will be l^{-d} . Assuming for simplicity $d = 1$, we get two limiting cases of $D = 0$ and $D = 1$, describing extreme events of single isolated points and a densely filled support of φ (Richtmyer, 1978. p. 51), respectively. In order to simulate a set with dimension D , therefore, one can generate a 1-dimensional cascade (e.g., Meneveau and Sreenivasan, 1987) and then at scale l select singularity level γ that corresponds to a given dimension D . Spatial distribution of points that are located on the intersection of the threshold $l^{-\gamma}$ (a line) and the cascade field φ_l will have the dimension D in the process of $l \rightarrow 0$.

The upper panel in Fig. 3 shows a 12-cascade p -model (Meneveau and Sreenivasan, 1987) with $p = 0.35$. For this simple model, there is an analytical relationship between the dimension D of the set and its singularity level γ . As an example, a threshold in the upper panel cuts a set of 79 clustered points shown in the lower part of the panel as small squares. Its dimension is estimated to be 0.3 (lower panel) and corresponds to $\gamma = 2/3$. The transition to a slope of -1 for large scales seen in the lower panel is due to a finite size of the interval in which points are located.

Similar to a 1-dimensional cascade model (that lies on a plane), one can use 2- and 3-dimensional cascades that lie in 3- and 4-dimensional spaces, respectively. The dimension of the set with singularity strength γ can be still described by Eq. (2). In case of a 3-dimensional cascade model, an intersection of the cascades by a 3-dimensional plane results in a set of points

randomly distributed in space. These points will be clustered in 3-dimensional space in a way similar to the ones clustered on a line in the upper panel of Fig. 3. The resulting degree of clustering is defined by the singularity strength γ and thus by the fractal dimension D . Figure 4 illustrates this process. The upper panel shows spatial distribution of more than 20,000 large drops as an intersection of a 3-dimensional plane and a 3-dimensional cascade model. It follows from scaling behavior of non-empty boxes (lower panel) that the mean number of drops N in volume V varies with V as V^D (Wiscombe et al., 2003; Knyazikhin et al., 2004). This conflicts with a fundamental assumption of radiative transfer, namely that the mean number of drops in volume V is proportional to V . The fractal dimension D of these drops is 0.56, which coincides with the one observed during a 2-hour flight on March 3, 2000 (see Fig. 2 and its analysis shown in Fig. 1).

Finally, Fig. 5 illustrates spatial distributions of 5,115 drops for two values of the fractal dimension. The “grey” drops are distributed uniformly. Their fractal dimension is 1; this is an implicit assumption behind most of the current radiative transfer theories in cloudy atmosphere. By contrast, the “black” drops are clustered and their spatial variation follows Eq. (1) with D close to 0.55. As a result, the frequency of occurrence of black drops along the line is lower than the frequency of occurrence of grey drops. However, the mean number of black drops in non-empty “boxes” is larger than that of grey drops.

Consider a “tube” with a cross-section thick enough to capture the 3-dimensional structure of drop spatial distribution. Since the distributions of the black (and grey) drops are isotropic by construction (i.e., there is no a preferential direction), any multiple-bend tube that is

long enough will show a spatial distribution statistically similar to that observed during the cloud IOP (Fig. 2). By statistical similarity here we understand that the number of large drop samples follows a power law (1) with exponents D close to $1/2$. Unfortunately, a simulated 3-dimensional spatial distribution of drops (8 cascades requires about 20 million points) doesn't provide us with a long enough scaling range to observe a power-law behavior similar to the one in Fig. 1. Instead, we have run a 1-dimensional 23-cascades model with the same fractal dimension $D = 0.56$. Figure 6 illustrates the results. In addition, a case of a perfectly random distribution of the same number of drops is also shown.

Thresholding multiplicative cascades is not the only way to simulate cloud drops whose spatial distribution follows Eq. (1). Another natural technique is to use an additive Levy flight (e.g., Mandelbrot, 1982, p. 132-143): a sequence of jumps that are statistically independent segments whose length follows the probability distribution

$$Prob(X > x) \propto x^{-\alpha} \quad (0 < \alpha < 2), \quad (3)$$

that is, the number of jumps exceeding x is a hyperbolic distribution with parameter α . Note that for Levy flights all moments of order $k > \alpha$ diverge. The limiting case of $\alpha = 2$ corresponds to a Gaussian distribution; thus its random walk corresponds to Brownian motion where all jumps are normally distributed. The case $\alpha = 1$ is the Cauchy distribution: the behavior is dominated by one or two large "jumps." Decreasing α makes the long segments longer and the short segments shorter, thus increasing clustering. An example of this distribution for simulating rain drops can

be found in Lovejoy and Mandelbrot (1985). For the relationship between a hyperbolic parameter α from (3) and a fractal dimension D defined in (1) see Mandelbrot (1982).

In general, the exponent D determines the type of the distribution. The probability theory distinguishes three classes, or types, of distributions; that is, absolutely continuous ($D = 1$); singular ($0 < D < 1$) and discrete ($D = 0$) distributions (e.g., Richtmyer, 1978, p. 260). Each of these classes contains an “infinite” number of distributions. A multiplicative turbulence cascade model and the additive Levy distribution used here are just two examples from the set of singular distributions. Their common feature is the exponent D ; the closer D is to 0 the closer are the values of the distribution function to the discrete set. This is a direct consequence of the Lebesgue (e.g., Richtmyer, 1978, p. 260) theorem on decomposition of the distribution and the Hausdorf-Besicovitch dimension (e.g., Barnsley, 1988, p. 202).

4. Summary and Discussion

Equation (1) provides a quantitative means for a size-dependent description of clustering and spatial distribution of drops. It states that the intensity of clustering is measured by the power-law exponent $0 < D < 1$. The smaller D , the larger the degree of clustering. When $D = 1$, cloud drops are not clustered and the number of drops in a volume is proportional to the volume. Equation (1) also allows us to develop a scale-invariant model of the spatial distribution of large drops that has the same drop size-dependent exponents as the ones observed. Below we discuss briefly the possible use of Eq. (1) and cloud drop models in cloud physics and radiation.

The spatial distribution of cloud drops, especially large drops, is not yet fully understood and remains controversial (see Pinsky and Khain, 2001 and references therein). Small-scale spatial correlation and clustering are important in cloud drop growth rate and can help explain of some fundamental problems in cloud physics. For example, Twomey (1976) suggested clustering (“pockets of high liquid water”) for explaining observed warm rain. Once a correct theory which predicts the observed power-law statistics is in hand, the strong clustering of larger drops falls out naturally from the statistics; no *deus ex machina* need be invoked to explain the clustering. Recently, McGray and Liu (2003) developed a new model for cloud drizzle formation that quantitatively explains how cloud turbulence (which governs clustering) enhances the growth of cloud droplets by both condensation and collection. In particular, they showed that once drops reach a critical radius of about $20 \mu\text{m}$ they can grow much faster through collection transforming cloud drops to drizzle size. Classical condensation theory was unable to explain the production of these drops because of their slow growth rate.

Since cloud turbulence governs clustering, the scale exponents $D(r)$ depend on the microscale properties of clouds determined by thermodynamic and fluid-mechanical interactions between droplets and surrounding air. However, the exponents have nothing to do with cloud macroscale structure. In other words, two clouds could “look” alike dynamically but have different microscale turbulence and different degrees of clustering; or they might “look” different dynamically but have similar microscale turbulence and thus the same degree of clustering.

To see the consequences of scaling behavior (1) on cloud radiative properties, let us assume for simplicity that a cloud consists of only two types of drops: small drops (subscript S) with $D_S = 1$ and large drops (subscript L) with $0 < D_L < 1$. The mean number, $n(r, V)$, of drops with radius r in a volume V is

$$n(r, V) = n_S(V)\delta(r-r_S) + n_L(V)\delta(r-r_L) \quad (4)$$

where

$$n_S(V) = \rho_S V^{D_S} = \rho_S V \quad (5a)$$

and

$$n_L(V) = \rho_L V^{D_L} . \quad (5b)$$

are the mean number of small and large drops in volume V , respectively. Here ρ_S and ρ_L are *volume-independent* (generalized) drop concentration [in number per $(\text{cm}^3)^D$, see Wiscombe et al., 2003 and Knyazikhin et al., 2004]. Substituting (4)-(5) into the definition of droplet effective radius r_e (e.g., Hansen and Travis, 1974) we get

$$r_e(V) = \frac{\rho_S V r_S^3 + \rho_L V^{D_L} r_L^3}{\rho_S V r_S^2 + \rho_L V^{D_L} r_L^2} . \quad (6)$$

It follows from (6) that for small scales, $r_e(V) \rightarrow r_L$ as $V \rightarrow 0$, while for large scales $r_e(V) \rightarrow r_S$ as $V \rightarrow \infty$. If one assumes $D_L = 1$, as does the conventional technique, we get $r_e(V) \equiv r_e$ which is typically much closer to r_S than to r_L since concentration of large drops is “negligible” compared to small ones ($\rho_L \ll \rho_S$). In other words, the conventional technique systematically

underestimates the effect of large drops at small scales. That is, the effective radius of a cloud with large drops distributed uniformly (grey dots in Fig. 5) is almost always smaller than the one for a cloud where the spatial distribution of large drops follows (1) with $D < 1$ (as black dots in Fig. 5). This suggests a partial explanation for the fact that r_e retrieved from satellites is usually larger than the one measured in situ (e.g., Dong et al. (2002) for the March 2000 ARM Cloud IOP, also Figs. 1 and 2).

With size dependent models of (realistic) spatial distributions of cloud drops in hand, the next logical step in understanding the radiative impact of correlation (or clustering) in the spatial distribution of large drops will be an accurate calculation of radiation fields in these modeled clouds. Knyazikhin et al. (2004) derived an equation that describes the attenuation of the radiance in clouds that have a spatial distribution of drops parameterized in terms of the exponent as in Eq. (1). They showed that the assumption of small-scale homogeneity of cloud drops ($D = 1$ in the parameterization (1)) underestimates the radiative effect of large drops, which can result in systematic underestimation of cloud optical distance. To confirm Knyazikhin et al. (2002, 2004) conclusions, the “first-principle” Monte Carlo method needs to be applied to the simulated clouds and compared with the uniform distribution of droplets. The results will be reported elsewhere.

Acknowledgments. This research was supported by the Department of Energy (under grant DE-AI02-95ER61961 to NASA’s GSFC) as part of the Atmospheric Radiation Measurement (ARM) program and by the NASA Radiation Science Program (under grant NNG04GF15G to

Boston University). ML was supported by the Department of Defense's "National Defense Science and Engineering Graduate Fellowship Program." He also thanks the Goddard Summer Student Program for its support of this research and his stay at NASA GSFC for the summer of 2003.

References

- Baker, B., 1992: Turbulent entrainment and mixing in clouds: A new observational approach. *J. Atmos. Sci.*, **49**, 387–404.
- Barnsley, M., 1988: *Fractals Everywhere*, Academic Press, San Diego (Ca), 402 pp.
- Brenguier, J.-L., T. Bourianne, A. Coelho, J. Isbert, R. Peytavi, D. Trevarin, and P. Wechsler, 1998: Improvements of droplet size distribution measurements with the Fast FSSP. *J. Atmos. Oceanic Technol.*, **15**, 1077–1090.
- Chhabra, A. B., C. Meneveau, R. V. Jensen, and K. R. Sreenivasan, 1989: Direct determination of the $f(\alpha)$ singularity spectrum and its application to fully developed turbulence, *Phys. Rev. A*, **40**, 5284-5294.
- Davis, A., Marshak, A., Gerber, H., and Wiscombe, W., 1999: Horizontal Structure of Marine Boundary-Layer Clouds from Cm– to Km–Scales. *J. Geophys. Res.* **104**, 6123-6144.
- Dong, X., P. Minnis, G. G. Mace, W. L. Smith Jr., M. Poellot, R. T. Marchan, and A. D. Rapp, 2002: Comparison of stratus cloud properties deduced from surface, GOES, and aircraft data during the March 2000 ARM Cloud IOP. *J. Atmos. Sci.*, **59**, 3265-3284.
- Hansen, J. E., and L. D. Travis, 1974: Light scattering in planetary atmospheres, *Space Science Reviews*, **16**, 527–609.
- Hobbs, P. V. and A. L. Rangno, 1985: Ice particles concentrations in clouds. *J. Atmos. Sci.*, **42**, 2523–2549.

- Jameson, A. R., A. B. Kostinski, and R. A. Black, 1998: The texture of clouds, *J. Geophys. Res.*, **103**, 6211–6119.
- Knyazikhin, Y., A. Marshak, W. J. Wiscombe, J. Martonchik, and R. B. Myneni, 2002: A missing solution to the transport equation and its effect on estimation of cloud absorptive properties, *J. Atmos. Sci.*, **59**, No.24, 3572-5385.
- Knyazikhin, Y., A. Marshak, W. J. Wiscombe, J. Martonchik, and R. B. Myneni, 2004: Influence of small-scale cloud drop size variability on estimation cloud optical properties, *J. Atmos. Sci.*, (submitted).
- Kostinski, A. B., and A. R. Jameson, 1997: Fluctuation properties of precipitation, 1. On deviations of single-size drop counts from the Poisson distribution, *J. Atmos. Sci.*, **54**, 2174-2186.
- Kostinski, A. B., and A. R. Jameson, 2000: On the spatial distribution of cloud particles, *J. Atmos. Sci.*, **57**, 901-915.
- Liu Y.G, and J. Hallett, 1998: On size distributions of cloud droplets growing by condensation: A new conceptual model. *J Atmos Sci.*, **55**, 527-536.
- Liu, Y., P. H. Daum, and J. Hallett, 2002: A generalized systems theory for the effect of varying fluctuations on cloud droplet size distribution. *J. Atmos. Sci.*, **59**, 2279-2290.
- Lovejoy, S., and B. B. Mandelbrot, 1985: Fractal properties of rain and a fractal model. *Tellus*, **37A**, 209–232.

- Mandelbrot, B., 1982. *The Fractal Geometry of Nature*, W.H. Freeman and Co., San Francisco, 460 pp.
- McGraw, R., and Y. Liu, 2003: Kinetic potential and barrier crossing: a model for warm cloud drizzle formation. *Phys. Rev. Lett.*, **90**, 018501-1–4.
- Meneveau, C., and K. R. Sreenivasan, 1987: Simple multifractal cascade model for fully developed turbulence. *Phys. Rev. Lett.*, **59**, 1424–1427.
- Pawłowska, H., and J.-L. Brenguier, 1997: Optimal nonlinear estimation for cloud particle measurements. *J. Atmos. Oceanic Technol.*, **14**, 88–104.
- Pinsky M., and A. P. Khain, 2001: Fine structure of cloud droplet concentration as seen from the Fast-FSSP measurements. Part I: Method of analysis and preliminary results. *J. Appl. Meteor.*, **40**, 1515–1537.
- Pinsky M., and A. P. Khain, 2003: Fine structure of cloud droplet concentration as seen from the Fast-FSSP measurements. Part II: Results of in situ observations. *J. Appl. Meteor.*, **42**, 65–73.
- Richtmyer, R. D., 1978: *Principles of Advanced Mathematical Physics*. V. 1, Springer –Verlag, New York, 422 pp.
- Schertzer, D., and S. Lovejoy, 1989: Generalized scale invariance and multiplicative processes in the atmosphere. *Pageoph*, **130**, 57-81.
- Shaw, R. A., A. B. Kostinski, and M. L. Larsen, 2002: Towards quantifying droplet clustering in clouds. *Quart. J. Roy. Meteor. Soc.*, **128**, 1043-1057.

Twomey, S., 1976: The effects of fluctuations in liquid water content on the evolution of large drops by coalescence. *J. Atmos. Sci.*, **33**, 720-723.

Wiscombe, W., Y. Knyazikhin, and A. Marshak, 2003. A new look into the treatment of small-scale drop variability in radiative transfer. In *Proceedings of the 13th Atmospheric Radiation Measurement (ARM) Science Team Meeting*, March 31 - April 4, 2003, Broomfield (Co) http://www.arm.gov/docs/documents/technical/conf_0304/wiscombe-wj.pdf.

Young, K. C, 1993: *Microphysical Processes in Clouds*. Oxford University Press, 427 pp.

Figure Captions

Figure 1. Number, $N(r,l)$, of FSSP samples containing drops with radii $r = 7\pm 2 \mu\text{m}$ (bin #4) and $r = 23\pm 2 \mu\text{m}$ (bin # 12) vs. scale l (see Knyazikhin et al., 2004) derived from data collected by an FSSP probe on board the University of North Dakota Citation aircraft during the ARM Cloud Intensive Operational Period (March, 2000). The data are publicly available at <http://iop.archive.arm.gov/arm-iop/2000/sgp/cloud/poellot-citation/>. While for small drops, $D \approx 1$, for large drops at scales between 80 m and 40 km the variation in $N(r,l)$ clearly follows a power law with an exponent $D = 0.56$.

Figure 2. Concentration of drops of radius $r = 7\pm 2 \mu\text{m}$ (bin #4) and $r = 23\pm 2 \mu\text{m}$ (bin #12) for the 2 hours of the same flight (March 3, 2000) as in Fig. 1. Note that small droplets (upper panel) almost uniformly fill the space; the set of points on the horizontal axis with positive concentration has a fractal dimension close to 1. In contrast, large drops (lower panel) are clustered; a fractal dimension of the set with positive concentration is 0.56.

Figure 3. The top panel is a simple log-binomial cascade model known in the literature as the p -model (Meneveau and Sreenivasan, 1987). 12 cascades with $p = 0.35$ are used. An example of a threshold with a singularity strength $\gamma = 2/3$ is shown as a dash line. Points on the horizontal axis at which values of the cascade field exceed the threshold are depicted in the top panel as small squares. There are 79 of them and they are obviously clustered. The lower panel illustrates a log-by-log plot of number of nonempty boxes of scale l needed to cover these 79 points versus the scale l . The small-scale slope gives the dimension D of the points. For this simple cascade

model an analytical relationship between fractal dimension D and the singularity γ can be found in Meneveau and Sreenivasan, (1987). According to this relationship $\gamma = 2/3$ corresponds to $d \approx 0.3$.

Figure 4. A simulated “cloud” piece with more than 2×10^4 (actually 21058) large drops. A 3-dimensional 8-cascade model with the total number of pixels $2^{24} \approx 2 \times 10^8$ was used. A 4-dimensional cutoff at a singularity level that gives fractal dimension $D = 0.56$ has been used to simulate the spatial distribution of drops (upper panel). Lower panel demonstrates a straight line on a log-log plot of number of nonempty boxes vs. scale, i.e., $N(l) \propto V^{-D} = l^{-3D}$. Note that the observed variation in $N(l)$ along the flight path for drops with radii $r = 23 \pm 2 \mu\text{m}$ exhibits similar behavior (Fig. 1).

Figure 5. An example of the space-filling properties of distributions with different fractal dimensions. Here are an equal amount of drops (total number of 5115) that are colored grey and black. The grey drops are distributed perfectly randomly throughout the space (having a fractal dimension close to 1) whereas the black particles are distributed in a such way that their fractal dimension is significantly less than 1 (between 0.5 and 0.55). The spatial distribution of black drops was simulated as an intersection of a 3-dimensional plane and a 3-dimensional 8-cascade model imbedded in a 4-dimensional space.

Figure 6. Scaling behavior of nonempty “boxes”, N , vs. scale l for a 1-dimensional cascade model with 23 cascades. A power-law behavior with a scaling exponent 0.56 is well established over at least 3 orders of magnitude. For comparison, the N vs. l curve for a perfectly random distribution of the same number of drops (142,680) is also shown. Note that at small scales ($l \rightarrow 0$), $N(l)$ is equal to the total number of drops (in this case, 142,680).

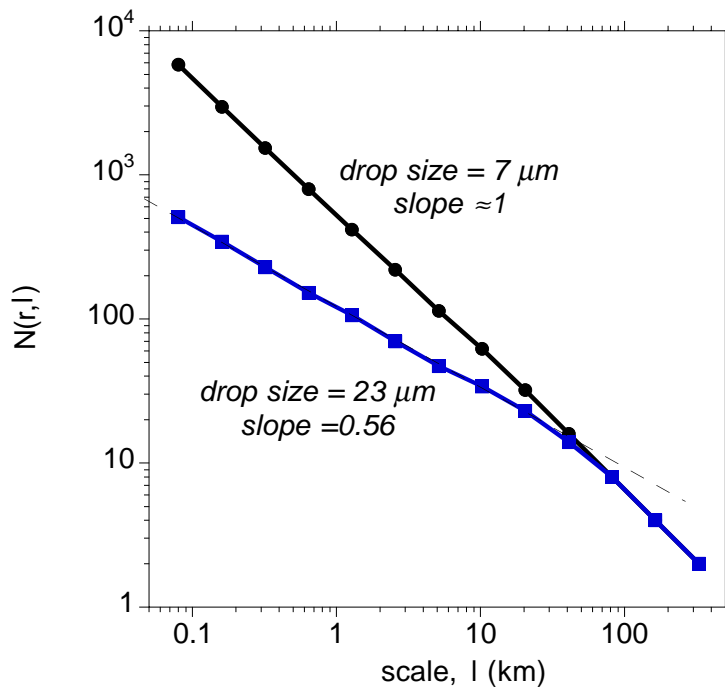


Figure 1. Number, $N(r,l)$, of FSSP samples containing drops with radii $r = 7 \pm 2 \mu\text{m}$ (bin #4) and $r = 23 \pm 2 \mu\text{m}$ (bin # 12) vs. scale l (see Knyazikhin et al., 2004) derived from data collected by an FSSP probe on board the University of North Dakota Citation aircraft during the ARM Cloud Intensive Operational Period (March, 2000). The data are publicly available at <http://iop.archive.arm.gov/arm-iop/2000/sgp/cloud/poellot-citation/>. While for small drops, $D \approx 1$, for large drops at scales between 80 m and 40 km the variation in $N(r,l)$ clearly follows a power law with an exponent $D = 0.56$.

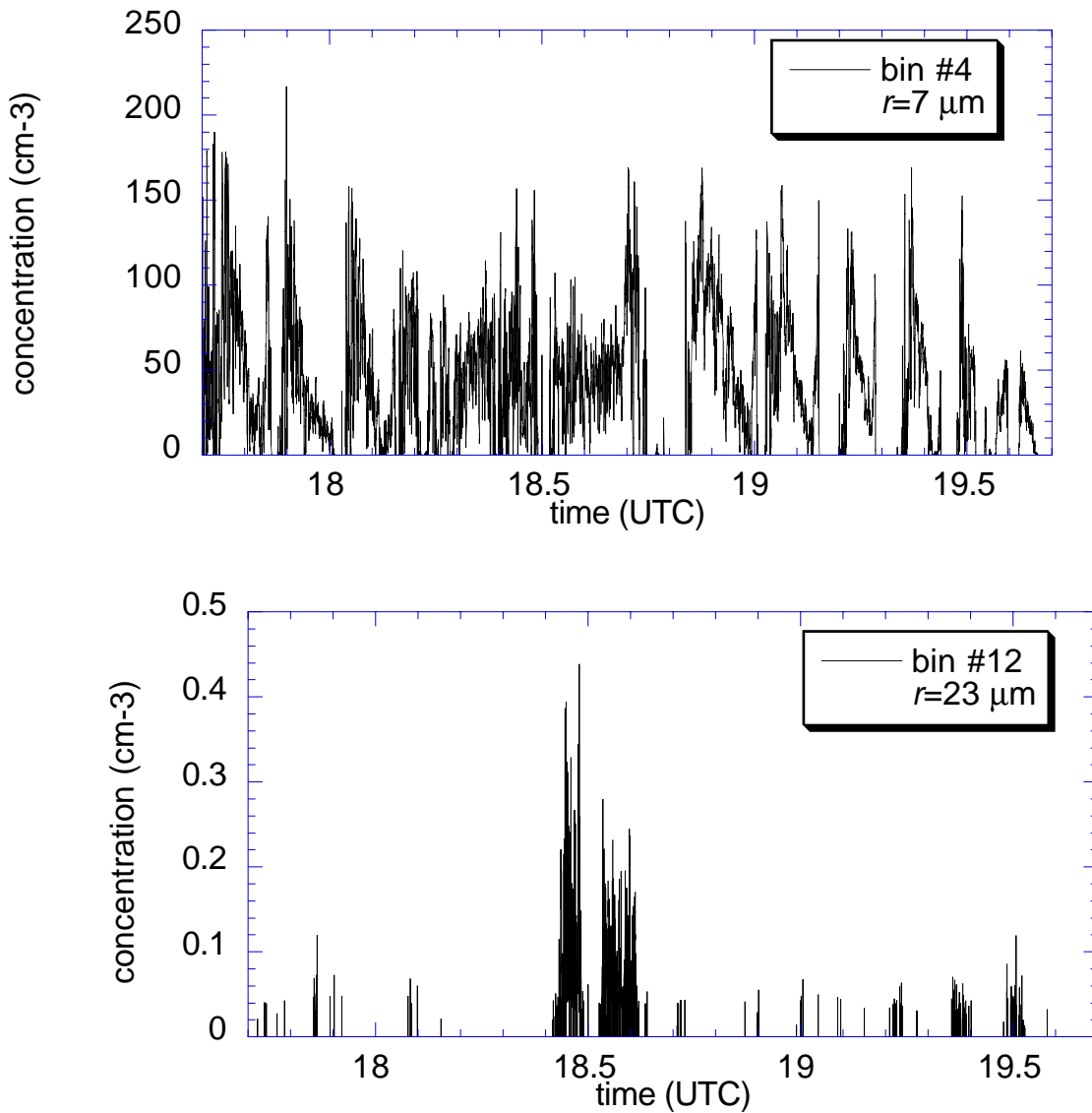


Figure 2. Concentration of drops of radius $r = 7 \pm 2 \mu\text{m}$ (bin #4) and $r = 23 \pm 2 \mu\text{m}$ (bin #12) for the 2 hours of the same flight (March 3, 2000) as in Fig. 1. Note that small droplets (upper panel) almost uniformly fill the space; the set of points on the horizontal axis with positive concentration has a fractal dimension close to 1. In contrast, large drops (lower panel) are clustered; a fractal dimension of the set with positive concentration is 0.56.

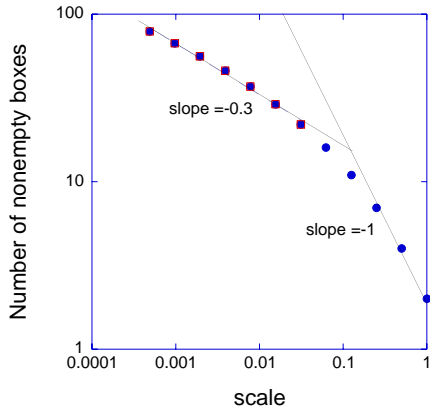
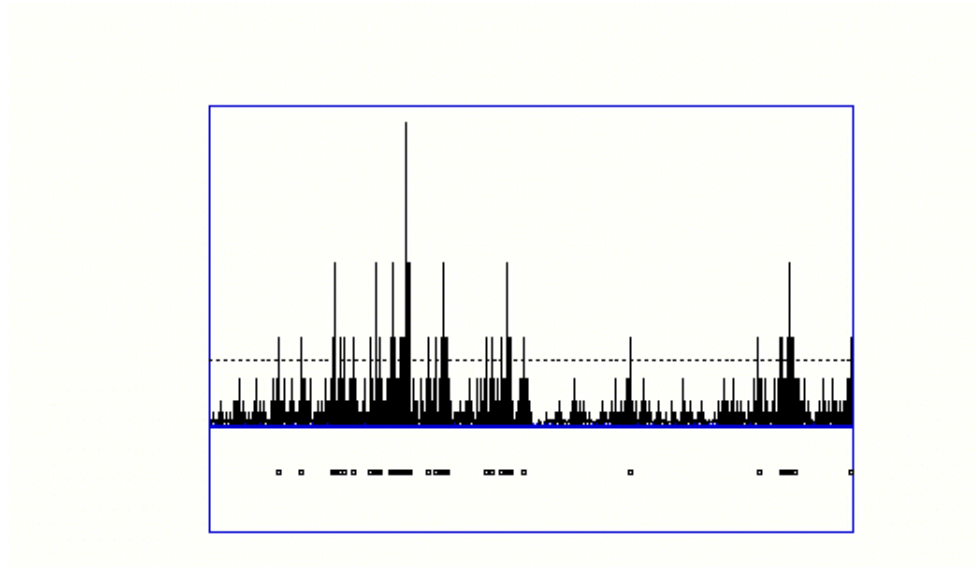


Figure 3. The top panel is a simple log-binomial cascade model known in the literature as the p -model (Meneveau and Sreenivasan, 1987). 12 cascades with $p = 0.35$ are used. An example of a threshold with a singularity strength $\gamma = 2/3$ is shown as a dash line. Points on the horizontal axis at which values of the cascade field exceed the threshold are depicted in the top panel as small squares. There are 79 of them and they are obviously clustered. The lower panel illustrates a log-by-log plot of number of nonempty boxes of scale l needed to cover these 79 points versus the scale l . The small-scale slope gives the dimension D of the points. For this simple cascade model an analytical relationship between fractal dimension D and the singularity γ can be found in Meneveau and Sreenivasan, (1987). According to this relationship $\gamma = 2/3$ corresponds to $D \approx 0.3$.

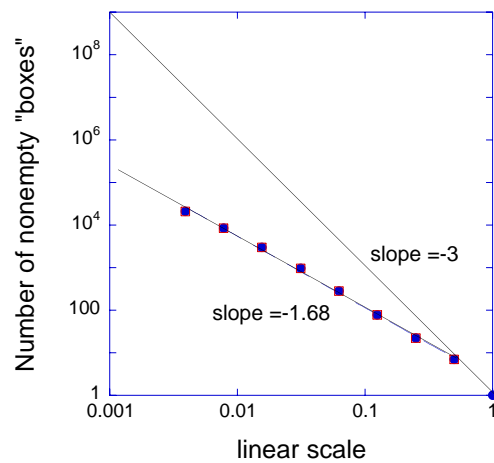
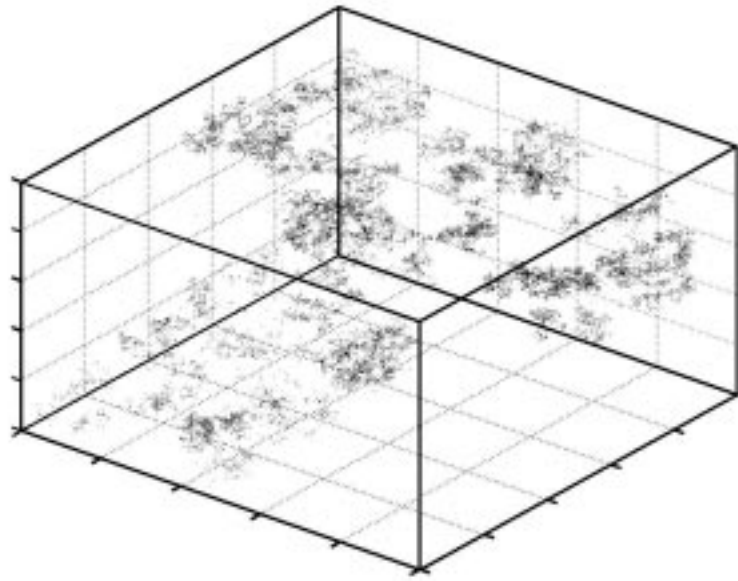


Figure 4. A simulated “cloud” piece with more than 2×10^4 (actually 21058) large drops. A 3-dimensional 8-cascade model with the total number of pixels $2^{24} \approx 2 \times 10^8$ was used. A 4-dimensional cutoff at a singularity level that gives fractal dimension $D = 0.56$ has been used to simulate the spatial distribution of drops (upper panel). Lower panel demonstrates a straight line on a log-log plot of number of nonempty boxes vs. scale, i.e., $N(l) \propto V^{-D} = l^{-3D}$. Note that the observed variation in $N(l)$ along the flight path for drops with radii $r = 23 \pm 2 \mu\text{m}$ exhibits similar behavior (Fig. 1).

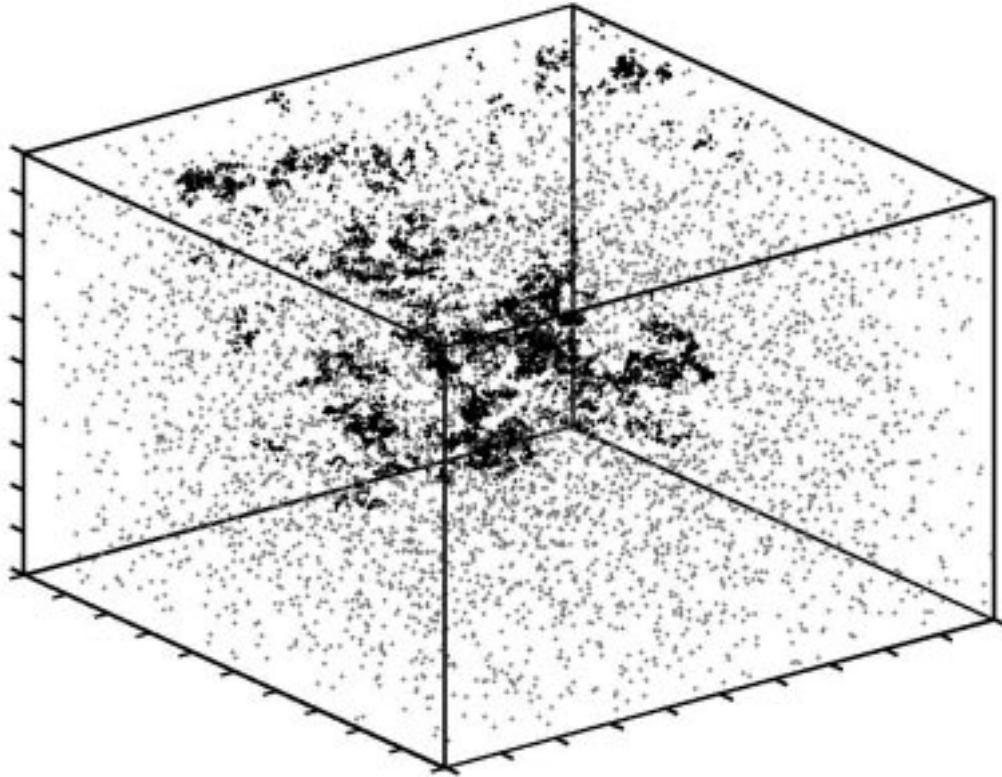


Figure 5. An example of the space-filling properties of distributions with different fractal dimensions. Here are an equal amount of drops (total number of 5115) that are colored grey and black. The grey drops are distributed perfectly randomly throughout the space (having a fractal dimension close to 1) whereas the black particles are distributed in a such way that their fractal dimension is significantly less than 1 (between 0.5 and 0.55). The spatial distribution of black drops was simulated as an intersection of a 3-dimensional plane and a 3-dimensional 8-cascade model imbedded in a 4-dimensional space.

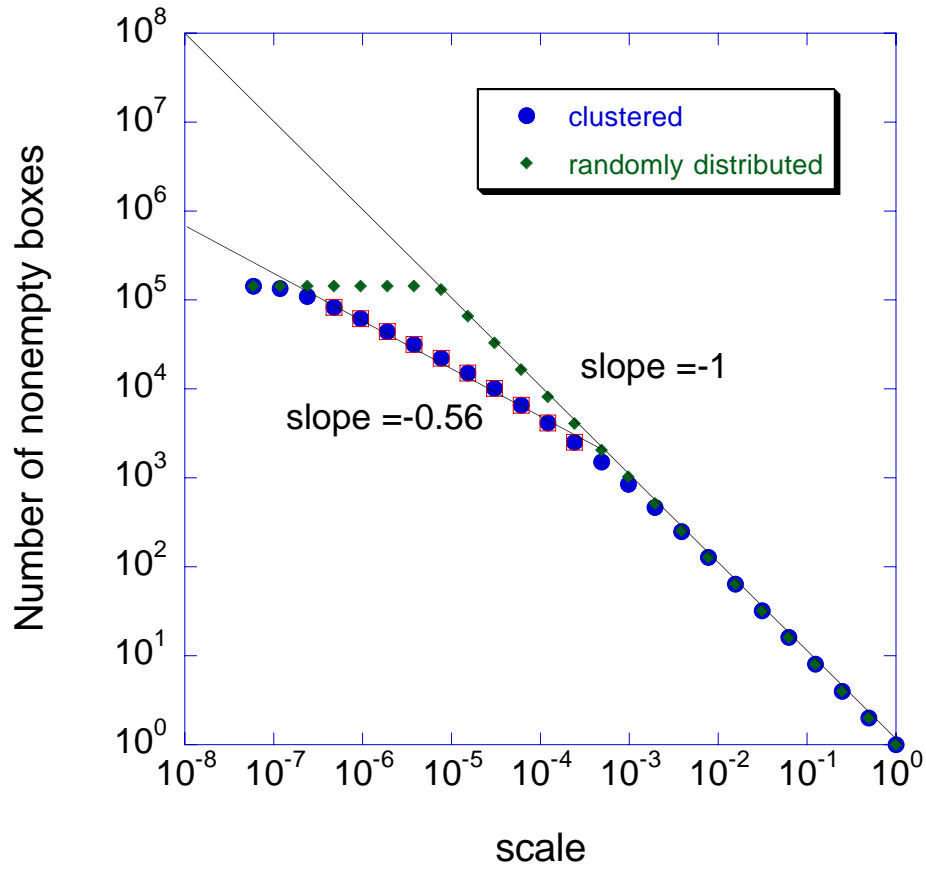


Figure 6. Scaling behavior of nonempty “boxes”, N , vs. scale l for a 1-dimensional cascade model with 23 cascades. A power-law behavior with a scaling exponent 0.56 is well established over at least 3 orders of magnitude. For comparison, the N vs. l curve for a perfectly random distribution of the same number of drops (142,680) is also shown. Note that at small scales ($l \rightarrow 0$), $N(l)$ is equal to the total number of drops (in this case, 142,680).